Synthesis and structural characterization of a diruthenium pentalene complex, [Cp*Ru(Cp*Ru)(2)B6H14(Cp*Ru)]

Benson Joseph, Subrat Kumar Barik, Soumya Kumar Sinha, Thierry Roisnel, Sundargopal Ghosh

Synthesis and structural characterization of a diruthenium pentalene complex, $[Cp^*Ru\{(Cp^*Ru)_2B_6H_{14}\}(Cp^*Ru)]$

BENSON JOSEPH,[a] SUBRAT KUMAR BARIK,[a] SOUMYA KUMAR SINHA,[a] THIERRY ROISNEL[b] and SUNDARGOPAL GHOSH*,[a]

[a]Department of Chemistry, Indian Institute of Technology Madras, Chennai 600036, India. Phone: (+91) 44 2257 4230, Fax: (+91) 44 2257 4202

E-mail: *sghosh@iitm.ac.in*
*For Correspondence

[b]Institut des Sciences Chimiques de Rennes, UMR 6226 CNRS-Ecole Nationale Supérieure de Chimie de Rennes-Université de Rennes 1, F-35042 Rennes Cedex, France.

E-mail: *Thierry.Roisnel@univ-rennes1.fr*

Abstract. Treatment of *nido*-[1,2-$(Cp^*Ru)_2(\mu\text{-}H)_2B_3H_7$], **1** with five equivalents of Te powder led to the isolation of diruthenium pentalene analogue $[(Cp^*Ru)\{(Cp^*Ru)_2B_6H_{14}\}(RuCp^*)]$, **2** and a metal indenyl complex $[(Cp^*Ru)_2B_2H_6C_6H_3(CH_3)]$, **3**. The $[(Cp^*Ru)_2B_6H_{14}]$ fragment in **2** may be considered as a true metal-boron analogue of η^5-η^5-pentalene ligand (C_8H_6) and $[(Cp^*Ru)B_2H_6C_6H_3(CH_3)]$ fragment in **3** is an analogue of η^5-indenyl ligand. The solid state X-ray structures were unambiguously determined by crystallographic analysis of compounds **2** and **3**. Further, the density functional theory (DFT) calculations were performed to investigate the bonding and the electronic properties of **2a** (Cp analogue of **2**). The frontier molecular orbital analysis of both **2a** and **2b** (Cp analogue of $[(Cp^*Ru)B_8H_{14}(RuCp^*)]$) reveals a lower HOMO–LUMO gap indicating less thermodynamic stability.

Keywords. Ruthenium; boron; pentalene; indenyl; metallaborane

1. Introduction

Over the past several decades, the significant research efforts in the field of transition metal boron chemistry have established several sandwich type metallaborane compounds.[1-4] In majority of these boron containing polyhapto π-ligand based sandwich complexes, metal atoms are sandwiched mainly by two types of polyhapto π-ligands (Chart 1).[1-4] The first such type of sandwich molecule $[(\eta^5\text{-}C_5H_5)FeB_5H_{10}]$ was reported by Grimes and coworkers in 1977.[1] Latter in 1984, Grimes reported $[(\eta^5\text{-}C_5H_5)CoB_4H_8]$[2] that showed the connection of isolobal analogy between (η^4-C_4H_4) and (η^4-B_4H_8) fragment. Fehlner and coworkers in 2005 reported a novel

dinuclear ruthenium-pentalene analogue ([(Cp*Ru)B_8H_{14}(RuCp*]).[3] Successively, they reported [(η^5-C_5Me_5Ir)B_5H_9] which was an analogue of [(η^5-C_5H_5)$_2$Fe], in which [B_5H_9]$^{2-}$ moiety is isoelectronic with the [η^5-C_5H_5]$^-$ ligand.[4]

As a part of our research efforts in the field of transition-metal-boron chemistry, we have isolated and characterized a wide range of metallaborane compounds of group 4-9[5-10] starting from novel boron-rich metallaboranes such as 15- and a 16-vertex rhodaborane clusters[10b-c] to complexes with a one boron for example, σ-borane,[9a-d] boryl,[9e] trimetallic bridging borylene[9f-g,10d] complexes. Recently, we have synthesized various metallaheteroboranes through the activation of heterocumulenes[9h], diaryl-dichalcogenide ligands[6a-c] or chalcogen powders.[7a-c] As a result, we have thermolysed the *nido*-[1,2-(Cp*Ru)$_2$(μ-H)$_2$$B_3H_7$] with Te powder that resulted in the formation of a diruthenium pentalene analogue **2** and a metal indenyl complex **3**. In this report, we describe the detailed structural characterization and bonding of these sandwich molecules.

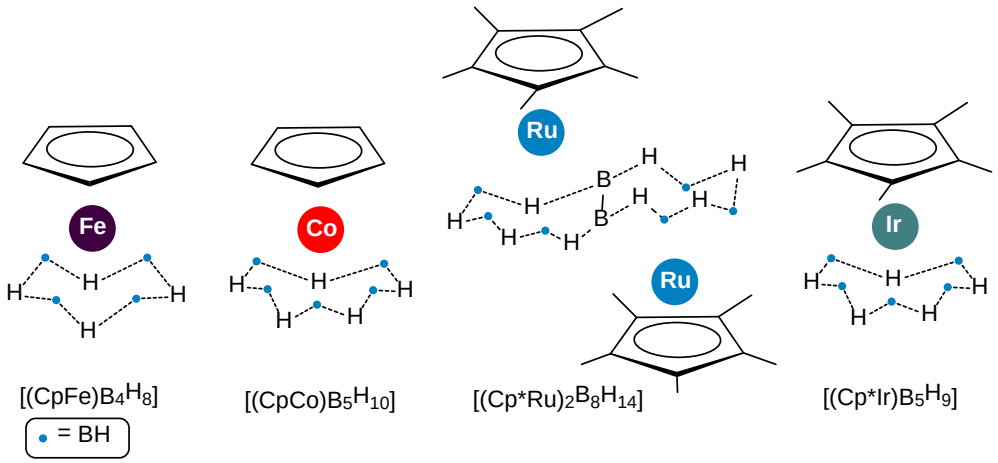

Chart 1. Selected examples of sandwich complexes containing polyhapto borane ligands analogous to organic π-ligands.

2. Experimental

2.1 *General considerations*

All the manipulations were conducted under an Ar/N_2 atmosphere using standard Schlenk techniques or glove box. Solvent were distilled prior to use under Argon. $LiBH_4$.THF 2.0 M, Cp*H, Tellurium powder (Aldrich) were used as received. [Cp*$RuCl_2$]$_2$[11] and *nido*-[1,2-(Cp*Ru)$_2$(μ-H)$_2$$B_3H_7$][12] was prepared according to the literature methods. The external reference [$Bu_4N(B_3H_8)$][13] for the ^{11}B NMR, was synthesized with the literature method. Preparative thin-layer chromatography was performed with Merck 105554 TLC Silica gel 60 F_{254}, layer thickness 250 µm on aluminum sheets (20 x 20 cm). The NMR spectra were recorded on a 500 MHz Bruker FT-NMR spectrometer. The residual solvent protons were used as reference (δ, ppm,

$CDCl_3$, 7.26; C_6D_6, 7.16), while a sealed tube containing $[Bu_4N(B_3H_8)]$ in $[D_6]$-benzene (δ_B, ppm, -30.07) was used as an external reference for the ^{11}B NMR. The Infrared spectra were recorded on a Jasco FT/IR-1400 spectrometer. Mass spectra were recorded on Bruker MicroTOF-II mass spectrometer in ESI ionization mode. The CV measurements were carried out on a CH potentiostat, model 668.

2.2 *Synthesis of compound **2***

Compound **1** (0.1 g, 0.19 mmol) was taken in a flame-dried Schlenk tube and dissolved in toluene (15 mL). The resulting solution was heated with five equivalents of Te powder (0.123 g, 0.95 mmol) at 80 °C for 18 hours. The reaction mixture was filtered through Celite using hexane. The filtrate was concentrated and the residue was chromatographed on silica gel TLC plates. Elution with a hexane/CH_2Cl_2 (90:10 *v/v*) mixture yielded orange **2** (0.09 g, 4.5%) and yellow **3**[14].

2: MS (ESI^+): *m/z* calculated for $[C_{40}H_{74}B_6Ru_4 + H^+]$, 1029.2, found, 1029.3; $^{11}B\{^1H\}$ NMR (160 MHz, d_6-benzene, 22 °C): δ = 21.5 (s, 1B), 14.2 (s, 1B), 11.5 (s, 1B), 9.5 (s, 1B), -1.9 (s, 1B), -30.6 (s, 1B); ^1H NMR (500 MHz, d_6-benzene, 22 °C): δ = 5.45 (br, BH_t), 4.82 (br, BH_t), 3.39 (br, BH_t), 2.96 (br, BH_t), 1.98 (s, 15H, Cp*), 1.91 (s, 15H, Cp*), 1.89 (s, 15H, Cp*), 1.82 (s, 15H, Cp*), -0.78 (br, 1H, B-H-B), -1.50 (br, 1H, B-H-B), -2.56 (br, 1H, B-H-B), -4.48 (br, 1H, B-H-B), -11.08 (br, 1H, Ru-H-B), -12.17 (br, 1H, Ru-H-B), -12.47 (br, 1H, Ru-H-B), -14.04 (br,1H, Ru-H-B), -11.85 (s, 1H, Ru-H-Ru), -14.66 (s, 1H, Ru-H-Ru); $^{13}C\{^1H\}$ NMR (125 MHz, d_6-benzene, 22 °C): δ = 95.2, 94.8, 87.5, 86.6 (s, C_5Me_5), 12.3, 12.2, 11.7, 10.5 (s, C_5Me_5); IR (DCM, cm^{-1}): 2962 (C-H), 2354, 2406 and 2480 (B-H_t). Raman (DCM, cm^{-1}): 289 (Ru-Ru).

2.3 *X-ray structure determination*

The crystal data for **2** and **3** were collected and integrated using a Bruker Axs kappa apex2 CCD diffractometer with graphite monochromated Mo-Kα (λ = 0.71073 Å) radiation at 150 K. The structures were solved by heavy atom methods using SHELXS-97[15a] or SIR92[15b] and refined using SHELXL-97.[15c]

Table1. Crystal data and structural refinement for compounds **2** and **3**

Compound	**2**	**3**
CCCDC no.	1828946	1828947
Empirical formula	$C_{40}H_{64}B_6Ru_4$	$C_{27}H_{42}B_2Ru_2$
Formula weight	1014.05	590.36
Temperature/K	150(2)	150(2)
Crystal system	triclinic	orthorhombic
Space group	*P*-1	$P2_12_12_1$
a/Å	11.1227(9)	11.4420(6)
b/Å	14.2888(11)	14.4265(9)
c/Å	15.6289(13)	16.3603(9)
α/°	70.293(3)	90
β/°	86.130(3)	90
γ/°	70.142(3)	90
Volume/$Å^3$	2196.3(3)	2700.6(3)
Z	2	4
$\rho_{calc}g/cm^3$	1.533	1.452
μ/mm^{-1}	1.375	1.13
F(000)	1020	1208
2θ range for data collection/°	5.834 to 49.998	6.122 to 54.948
Reflections collected	28291	15672
zIndependent reflections	7709 [R_{int} = 0.0606, R_{sigma} = 0.0614]	6158 [R_{int} = 0.0551, R_{sigma} = 0.0629]
Goodness-of-fit on F^2	1.163	1.104
Final R indexes [I>=2σ (I)]	R_1 = 0.0595, wR_2 = 0.1356	R_1 = 0.0453, wR_2 = 0.0900
Final R indexes [all data]	R_1 = 0.0780, wR_2 = 0.1495	R_1 = 0.0551, wR_2 = 0.0939

2.4 *Computational details*

Quantum chemical calculations were performed on compounds **2a**, **2b** and **3a** (Cp analogues of **3** *nido*-[$(Cp^*Ru)_2B_2H_8C_6H_3(CH_3)$]) using density functional theory (DFT) as implemented in the Gaussin09 package.[16] The calculations were carried out with the Cp analogue compounds instead of Cp* in order to save computing time. Without any symmetry constraints, all the geometry optimizations were carried out in gaseous state, (no solvent effect) using PBE0 functional[17] in combination with triple-ζ quality basis set Def2-TZVP. The calculated ^{11}B chemical shielding values, determined at the PBE0/Def2-TZVP level of calculations, were referenced to B_2H_6 (PBE0/Def2-TZVP, B shielding constant 85.9 ppm), and these chemical shift values (δ) were then converted to the standard $BF_3{\cdot}OEt_2$ scale using the experimental value of +16.6 ppm for

B_2H_6. The ^1H chemical shifts were referenced to TMS ($SiMe_4$). The computation of the NMR shielding tensors employed gauge-including atomic orbitals (GIAOs),[18] using the implementation of Schreckenbach, Wolff, Ziegler, and co-workers.[19] The ChemCraft package[20] was used for the visualizations. The two-dimension electron density and Laplacian electronic distribution plots were generated using Multiwfn package.[21]

3. Results and Discussion

3.1 *Synthesis of [(Cp*Ru){(Cp*Ru)$_2$B$_6$H$_{14}$}(RuCp*)],* ***2***

As shown in Scheme 1, the thermolysis of *nido*-**1** with five equivalents of Te powder yielded a moderately air stable solid **2**. Compound **2** isolated as orange solid in its purest form by thin-layer chromatography (TLC) and characterized by $^{11}B\{^1H\}$, ^1H and $^{13}C\{^1H\}$ NMR, IR spectroscopy and a single-crystal X-ray diffraction study. In parallel to the formation of compound **2**, reaction also yielded compound **3** in very less yield.[14] Compound **3** was characterised with limited spectroscopic data and a single-crystal X-ray diffraction analysis.

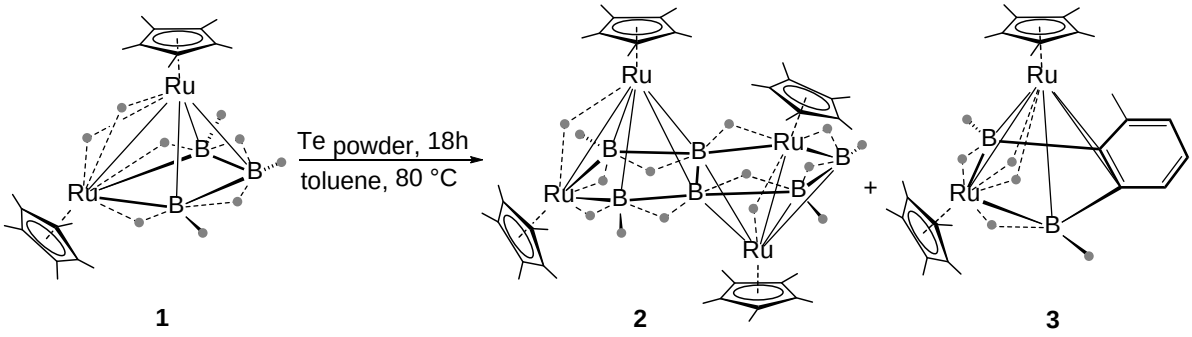

Scheme 1. Synthesis of compounds **2** and **3**.

The solid-state X-ray structure of **2**, shown in Figure 1, can be viewed as a fused structure in which two diruthenaborane cages fused in a transoid fashion with two common boron atoms, to generate a planar Ru_2B_6 fragment. The framework is analogous to that of isoelectronic dinuclear pentalene complexes [Cp*M(C_8H_6)MCp*], (M = Fe or Ru)[22] and [(Cp*Ru)(B_8H_{14})(RuCp*)][3] (Chart 2). In compound **2** the ruthenium atoms are bonded symmetrically to the Cp* ligands. The average Ru-B distance is found to be larger (d_{Ru-B} 2.228 Å) as compared to [(Cp*Ru)B_8H_{14}(RuCp*)] (d_{Ru-B} 2.15 Å). The average distance between two Ru is 2.837 Å. As shown in Figure 1, two Ru atoms (Ru2 and Ru3) are bridged by Cp* and [(Cp*Ru)$_2$B$_6$H$_{14}$] fragment, in which the ends of B_4H_x (x = 6 or 8) are bonded by two Ru atoms (Ru1 and Ru4) forming cyclic metal-boron rings. These cyclic RuB_4H_x (x = 6 or 8) units are fused by a B-B bond (B3-B6) resulting a fused dimetallacycle. The B6-Ru1-B1-B2-B3 ring is puckered with the Ru1 lying 0.128 Å out of the least square plane defined by boron atoms B1-B2-B3-B6 (mean

deviation from the plane = 0.045 Å). Similarly, in the Ru4 B6-B5-Ru4-B4-B3 ring the Ru4 lies 0.528 Å out of the least square plane defined by boron atoms B6-B5-B3-B4 (mean deviation from the plane = 0.003 Å).

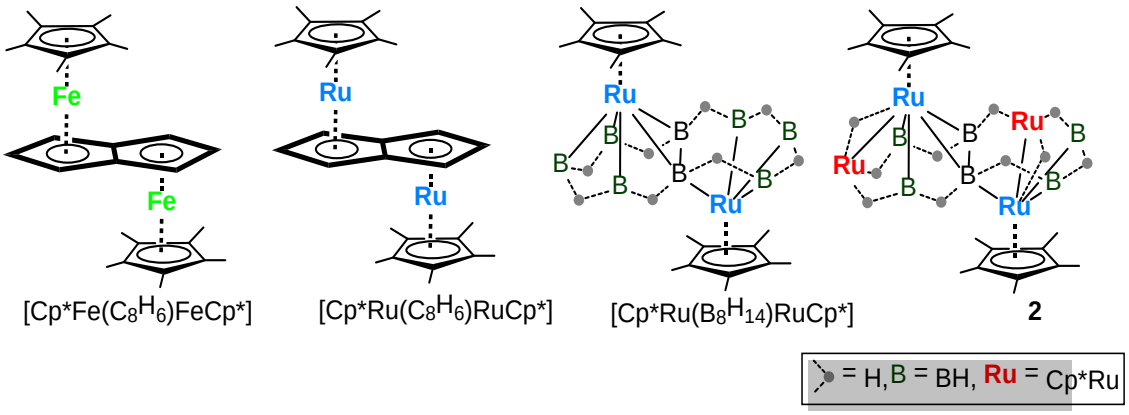

Chart 2. Dimetala pentalene complex [Cp*M(pentalene)MCp*] (M = Fe and Ru), pentalene analogue [Cp*Ru(B_8H_{14})RuCp*] and a metallaborane analogue of diruthenium pentalene, **2**.

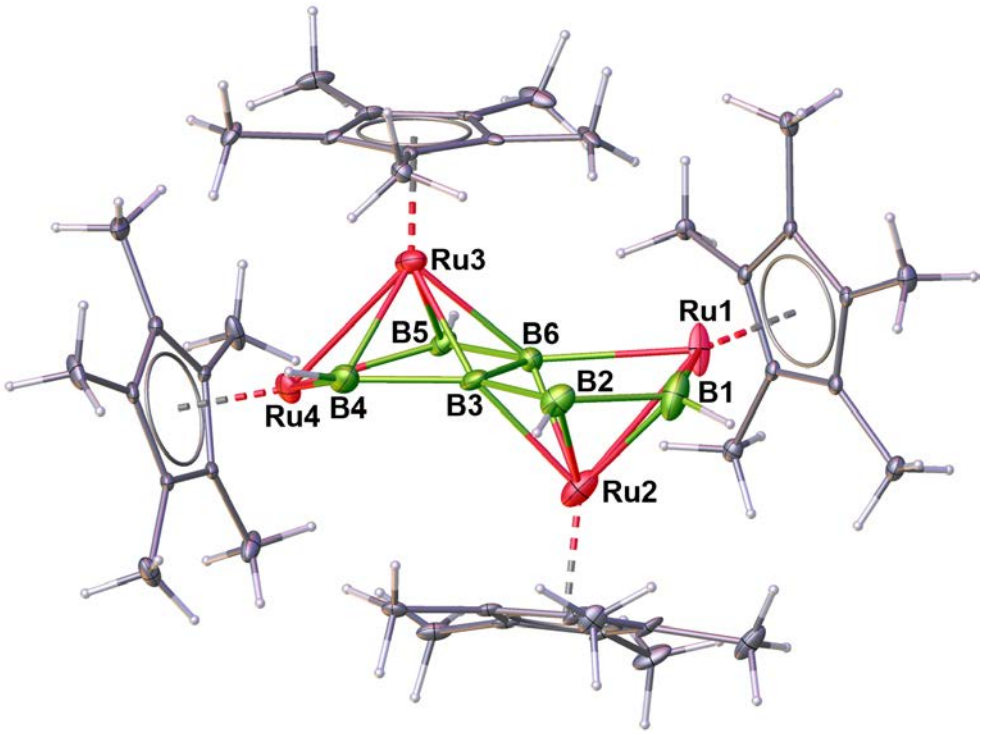

Figure 1. Molecular structure of compound **2**. Selected interatomic distances (Å) and angles (°): Ru1-Ru2 2.854(7), Ru3-Ru4 2.821(5), Ru1-B6 2.402(10), Ru1-B1 2.99(13), B1-B2 1.811(14), B3-B6 1.789(12), B1-Ru1-B6 81.0(4), B2-B3-B4 135.7(7), Ru1-B6-B5 133.9(5).

Consistence with the X-ray structure determination, the $^{11}B\{^1H\}$ NMR spectrum reveals six different resonances (δ = 21.58, 14.23, 11.59, 9.53, -1.95 and -30.66 ppm) reflecting the lack of

symmetry in the molecule. In addition to Cp* protons, the ^{1}H NMR spectrum of **2** shows up-field resonances at δ = -0.78, -1.50, -2.56 and -4.48 for B-H-B, -11.08, -12.17, -12.47 and -14.04 for B-H-Ru and -11.85 and -14.66 ppm for the presence of Ru-H-Ru protons. Assignment of the Ru-Ru stretching vibration in compound **2** is evidenced by a single resonance-enhanced band at 289 cm^{-1}, which falls within the reported range.[23]

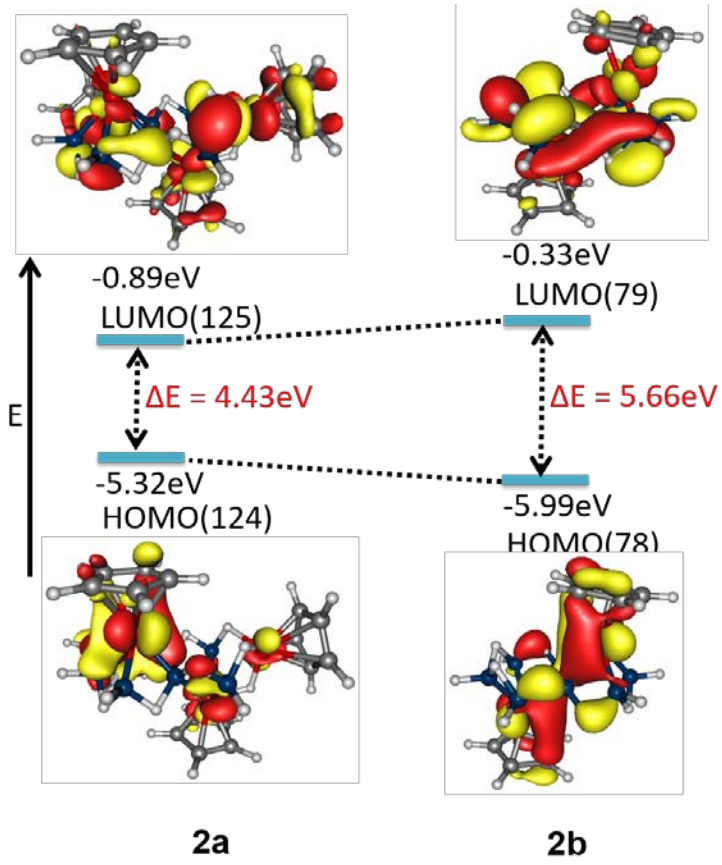

Figure 2. Frontier molecular orbitals of **2a** and **2b** (isocontour value ± 0.03 [e/Bohr^{3}]$^{1/2}$).

To gain some insight into the electronic structure and bonding nature of **2a (**Cp analogue of **2**), we carried out the density functional theory (DFT) calculations[16] and compared with **2b**. The optimized structure of **2a** (Figure S13 and Table S1) is in good match with its X-ray structure. Further, the DFT calcultaions helped us to confirm the position of the bridging hydrogen atoms that could not be located by X-ray diffraction studies. The DFT computed energy gap between the highest occupied molecular orbital (HOMO) and the lowest unoccupied molecular orbital (LUMO) for **2a** of 4.43 eV at PBE0 level is consistent with its high thermodynamic stability. However, the HOMO–LUMO gap for **2a** is much lesser than its parent metallaborane **2b** (5.66 eV). This led us to compare their MO diagrams (Figure 2). Analyses of the frontier orbitals for **2a** reveals a significant increase in HOMO energy (ca. 0.67 eV) and decrease in LUMO energy (ca.

0.56 eV) with respect to **2b**. Consequently, it leads to the decrease in HOMO–LUMO gap of **2a** compared to **2b** (Figure 2). Previous theoretical calculations on compound **2b** showed that the LUMO of $B_8H_{14}^{2-}$, which is essentially vacant orbitals cantered at $B_8H_{14}^{2-}$ ligand, is destabilized and higher in energy due to the electropositive nature of B.[24] In contrast, the presence of two 2 electron donor {Cp*RuH} fragments in the central $[(Cp^*Ru)_2B_6H_{14}]^{2-}$ ligand of **2a** destabilizes the HOMO and stabilizes the LUMO, resulting in a smaller HOMO/LUMO gap of **2a** (compared to **2b**). This may be attributed to the presence of electron rich {Cp*RuH} fragments compared to the BH units.

To understand the bonding of the nearly planar $[Cp^*Ru_2B_6H_{14}]^{2-}$ unit and the nature of Ru-B and B-B bonding in **2a**, the topological analyses[25] were carried out. As shown in Figure 3, the results show an area of charge concentration along each Ru-B and B-B bonds in $[Ru_2B_6]$ plane indicating the σ/π delocalized bonds between Ru and B atoms. In addition, the boron-metal interaction has more covalent character as compared to B-B bonds in **2a**. This is also indicated by higher values of the electron density (ρ) and a negative value of the energy density [$H(r)$] at bcps (Table S3).

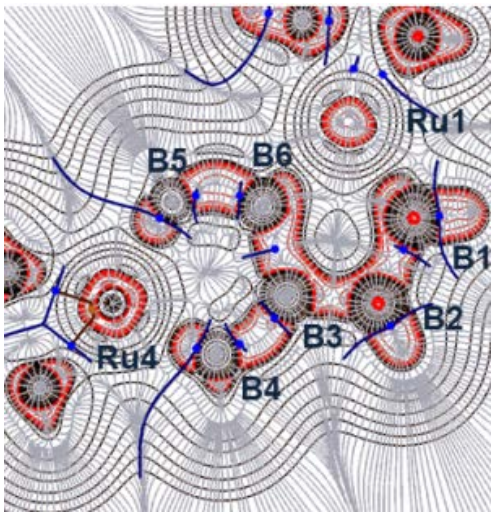

Figure 3. Contour line diagram of the Laplacian of the electron density, $\nabla^2\rho(r)$ of **2a** in the plane of $[Ru_2B_6]$ generated using the Multiwfn program package at the PBE0/Def2-TZVP level of theory. Solid red lines show areas of charge concentration ($-\nabla^2\rho(r) > 0$), while dashed black lines indicate areas of charge depletion ($-\nabla^2\rho(r) < 0$). Solid brown and blue lines indicate bond paths and zero-flux-surfaces, respectively, and blue dots indicate bond critical points (BCPs).

Compound **2** is a redox active molecule and which has been concluded from its cyclic voltammetric studies. The cyclic voltammogram of $[Cp^*Ru(C_8H_6)RuCp^*]$ exhibits one reversible oxidation wave and an irreversible wave at 0.29 V higher potential.[22b] The irreversible behaviour

is attributed to the oxidation reaction of the Cp* ligand, analogous to the behaviour of [Cp^*_2Ru] on oxidation. Compound **2** in a similar way exhibits three successive one-electron oxidations with the first two are separated by approximately 0.4 V while the 2nd and 3rd potentials are separated by 0.23 V. The first redox event $\mathbf{2}^0/\mathbf{2}^+$is quasi-reversible, but the second and third oxidations $\mathbf{2}^+/\mathbf{2}^{2+}$and $\mathbf{2}^{2+}/\mathbf{2}^{3+}$ are irreversible as shown by the lack of a return wave. The cyclic voltammogram of **2** is similar to that of $[(Cp^*Ru)B_8H_{14}(RuCp^*)]$[3] that shows two successive one-electron oxidations separated by approximately 0.8V (Figure S5 in SI).

3.2 *Solid state X-ray structure of **3***

Although compounds **2** and **3** were isolated from same reaction, all of our attempts to reproduce **3** were failed. However, with the limited spectroscopic data and an X-ray crystallographic analysis, we have characterized compound **3**. The $^{11}B\{^1H\}$ chemical shifts appeared at δ = -16.8 and -19.2 ppm with equal intensity arise from the two different boron environments. The ^1H NMR spectrum of **3** displayed two signals (δ = 1.87 and 1.51 ppm) corresponding to Cp* protons in 1:1 ratio. Further, it predicts the presence of three up-fielded resonances at δ = -10.84, -11.16 and -12.23 ppm. These observed up-fielded chemical shifts may be due to the presence of Ru-H-B and Ru-H-Ru hydrogens.

The solid-state X-ray structure of compound **3** may be considered as an eight-sep *nido*-$[(Cp^*Ru)_2B_2H_8C_6H_3(CH_3)]$ cluster (Figure 4). Compound **3** ($[(Cp^*Ru)_2B_2H_8C_6H_3(CH_3)]$) can be viewed as an edge fused ruthenaborane cluster in which a toluene ring being fused to a pentagonal pyramidal ring $Ru_2B_2C_2$. The structure of **3** is analogous to the isoelectronic ruthenium indenyl complex with a central indenyl ligand $[(\eta^5\text{-}C_5R_5)Ru(\eta^5\text{-}C_9H_7)]$ (R = Me).[26] The C-C bond length in **3** that is fused with the pentagonal pyramid ring is about 1.43 Å, which can be considered to have a partial double bond character. The respective C-C bond in **3** is slightly longer than the C=C bond length of toluene (1.40 Å), but shorter as compared to similar reported indenyl compounds,[27] which indeed longer than normal C=C length (1.33 Å). The Ru-Ru bond distance (2.9578 Å) is considerably longer than the reported diruthena-boranes[12,28] The RuB_2C_6 fragment in **3** is a true analogue of the η^5-indenly ligand and this further illustrates the similarity of the properties of boron and its immediate neighbour carbon and their tendency to form similar structures by using the concept of isolobal analogy.[29]

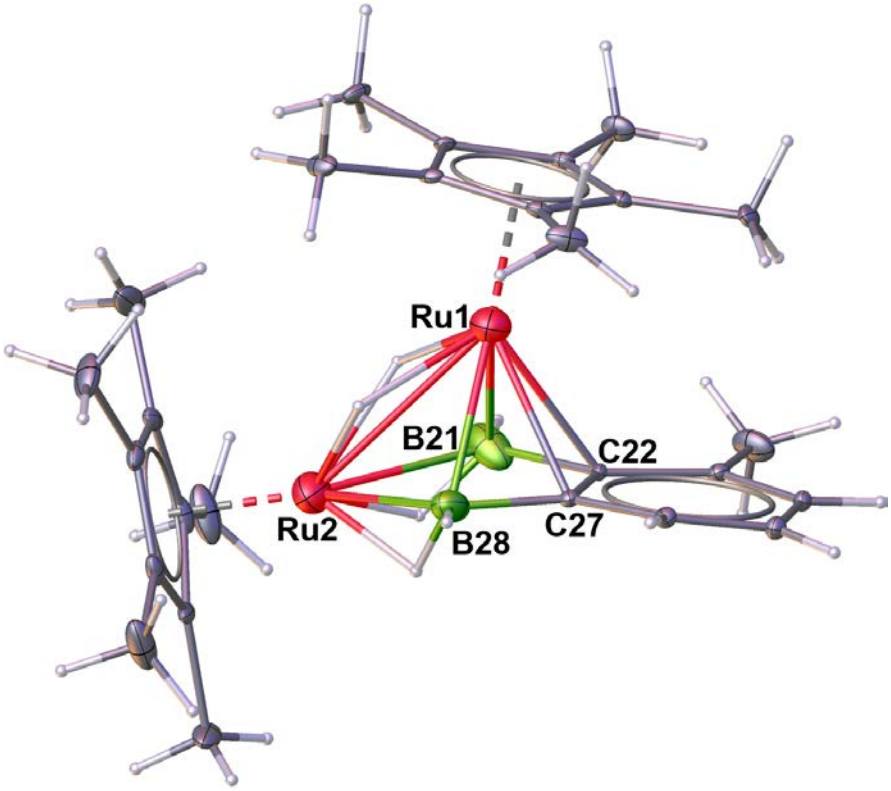

Figure 4. Molecular structure of compound **3**. Selected bond distances (Å) and angle (°): Ru1-Ru2 2.9578(8), Ru1-B21 2.349(12), Ru2-B21 2.391(11), Ru2-B28 2.386(10) C22-C27 1.43(3) Ru1-C22-B21 71.00(8), B21-Ru2-B28 76.4(4), B21-C22-C27 117.7(15), and C23-C22-C27 120.6 (17).

4. Conclusions

In this article, we have synthesised and structurally characterized the metallaborane analogue of diruthena pentalene and an indenyl complex. Diruthena pentalene complex **2** is a notable entry in to the class of pentalene complexes containing main group and transition metals. On the other hand, compound **3** that contains a $\{RuB_2C_6\}$ fragment is a true analogue of η^5-indenyl ligand. Theoretical calculations adequately explained the electronic structure of **2**. Further we have demonstrated that the HOMO-LUMO gap decreases when two of the BH fragments in the parent molecule were replaced by two 2 electron {Cp*RuH} fragments.

Supplementary Information (SI)

Supplementary data contains the X-ray crystallographic files in CIF format for **2** and **3**, CCDC 1828946 (**2**) and 1828947 (**3**) for this work. These data can be obtained free of charge from the Cambridge Crystallographic Data Centre via www.ccdc.cam.ac.uk/data_-request/cif. All additional information pertaining to characterization of the complexes **2-3** using ESI-MS technique, IR spectra and multinuclear NMR spectra (Figure S1 - Figure S8), computational details are given in the Supplementary Information available at www.ias.ac.in/chemsci.

Acknowledgments

Generous support of the Council of Scientific & Industrial Research, CSIR (Project No. 01(2837)/15/EMR-II), New Delhi, India, is gratefully acknowledged. B.J. and S.K.B. thank UGC and IIT Madras for research fellowships. We are very thankful to Dr. Bijan Mondal for scientific discussion. We thank Dr. Babu Varghese (SAIF, IIT Madras) for X-ray data analysis. IIT Madras is gratefully acknowledged for computational facilities.

References

1. Weiss R and Grimes R N, 1977 New ferraboranes. structural analogs of hexaborane(10) and ferrocene. A complex of cyclic $B_5H_{10}^-$, a counter part of $C_5H_5^-$ *J. Am. Chem. Soc.* **99** 8087
2. Venable T L, Sinn E and Grimes R N 1984 1-[(η^5-C_5R_5)Co]B_4H_8(R = H or Me) sandwich complexes containing a square cyclic $B_4H_8^{2-}$ ligand analogous to $C_4H_4^{2-}$: Structural and spectroscopic studies *J. Chem. Soc. Dalton Trans*. 2275
3. Ghosh S, Noll B C and Fehlner T P 2005 Borane mimics of classic organometallic compounds: $[(Cp^*Ru)B_8H_{14}(RuCp^*)]^{0+}$, Isoelectronic analogues of dinuclear pentalene complexes *Angew. Chem. Int. Ed.* **44** 6568
4. Ghosh S, Noll B C and Fehlner T P 2008 Expansion of iridaborane clusters by addition of monoborane. Novel metallaboranes and mechanistic detail *Dalton Trans*. 371
5. (a) De A, Zhang Q-F, Mondal B, Cheung L F, Kar S, Saha K, Varghese B, Wang L-S and Ghosh S 2018 $[(Cp_2M)_2B_9H_{11}]$ (M = Zr or Hf) early transition metal 'guarded 'heptaborane with strong covalent and electrostatic bonding *Chem. Sci*. **9** 1976

   (b) Ghosh S, Rheingold A L. and Fehlner T P 2001 Metallaboranes of the earlier transition metals. An arachno nine-vertex, nine-skeletal electron pair rhenaborane of novel shape: importance of total vertex connectivities in such systems *Chem.Commun*.895
6. (a) Roy D K, Bose S K, Geetharani K, Chakrahari K K V, Mobin S M and Ghosh S 2012 Synthesis and structural characterization of new divanada- and diniobaboranes containing chalcogen atoms *Chem. Eur. J.* **18** 9983

   (b) Dhayal R S, Chakrahari K K V, Varghese B, Mobin S M and Ghosh S 2010 Chemistry of Molybdaboranes: Synthesis, structures, and characterization of a new class of open-cage dimolybdaheteroborane clusters *Inorg. Chem.***49** 7741

   (c) Bose S K, Geetharani K, Ramkumar V, Varghese B and Ghosh S 2010 Chemistry of Vanadaboranes: Synthesis, structures, and characterization of organovanadium sulfide clusters with disulfido linkage *Inorg. Chem.* **49** 2881

(d) Bose S K, Geetharani K, Varghese B and Ghosh S 2010 Unusual organic chemistry of a metallaborane substrate: Formation of tantalaborane complex with bridging acyl group (μ-η^2) *Inorg. Chem.* **49** 6375

(e) Bose S K, Geetharani K and Ghosh S 2011 C–H Activation of arenes and heteroarenes by early transition metallaborane *Chem. Commun*. **47** 11996

(f) Bose S K, Geetharani K, Varghese B and Ghosh S 2011 Condensed Tantalaborane clusters: Synthesis and structures of $[(Cp^*Ta)_2B_5H_7\{Fe(CO)_3\}_2]$ and $[(Cp^*Ta)_2B_5H_9\{Fe(CO)_3\}_4]$ *Inorg. Chem.* **50** 2445

(g) Geetharani K, Krishnamoorthy B S, Kahlal S, Mobin S M, Halet J-F and Ghosh S 2012 Synthesis and characterization of hypoelectronic Tantalaboranes. Comparison of the geometric and electronic structures of $[(Cp^*TaX)_2B_5H_{11}]$ (X = Cl, Br and I) *Inorg. Chem*. **51** 10176

(h) Bose K, Geetharani K, Sahoo S, Reddy K H K, Varghese B, Jemmis E D, and Ghosh S 2011 Synthesis, characterization, and electronic structure of new type of heterometallic boride clusters *Inorg. Chem.* **50** 9414

7. (a) Sahoo S, Mobin S M and Ghosh S 2010 Direct insertion of Sulfur, Selenium and Tellurium atoms into metallaborane cages using chalcogen powders *J. Organomet. Chem.* **695** 945

(b) Thakur A, Sao S, Ramkumar V and Ghosh S 2012 Novel class of heterometallic cubane and boride clusters containing heavier group 16 elements *Inorg. Chem.* **51** 8322

(c) Geetharani K, Bose S K, Sahoo S, and Ghosh S 2011 A family of heterometallic cubane-type clusters with an exo-$Fe(CO)_3$ fragment anchored to the cubane *Angew. Chem. Int. Ed.* **50** 3908

(d) Geetharani K, Bose S K, Pramanik G, Saha T K, Ramkumar V and Ghosh S 2009 An efficient route to group 6 and 8 metallaborane compounds: Synthesis of *arachno*-$[Cp^*Fe(CO)B_3H_8]$ and *closo*-$[(Cp^*M)_2B_5H_9]$ (M = Mo, W) *Eur. J. Inorg. Chem*. 1483

(e) Roy D K, Mondal B, Shankhari P, Anju R S, Geetharani K, Mobin S M and Ghosh S 2013 Vertex-fused metallaborane clusters: Synthesis, characterization and electronic structure of $[(\eta^5\text{-}C_5Me_5Mo)_3MoB_9H_{18}]$ *Inorg. Chem.* **5** 6705

(f) Dhayal R S, Sahoo S, Reddy K H K, Mobin S M, Jemmis E D and Ghosh S 2010 Vertex-fused metallaborane clusters: synthesis, characterization and electronic structure of $[(\eta^5\text{-}C_5Me_5Mo)_3MoB_9H_{18}]$ *Inorg. Chem.* **49** 900

(g) Sahoo S, Reddy K H K, Dhayal R S, Mobin S M, Ramkumar V, Jemmis E D and Ghosh S 2009 Chlorinated hypoelectronic dimetallaborane clusters: synthesis, characterization, and

electronic structures of $(\eta^5\text{-}C_5Me_5W)_2B_5H_nCl_m$ (n = 7, m = 2 and n = 8, m = 1) *Inorg. Chem.* **48** 6509

8. Geetharani K, Bose S K, Sahoo S, Varghese B, Mobin S M and Ghosh S 2011 Cluster expansion reactions of group 6 and 8 metallaboranes using transition metal carbonyl compounds of groups 7-9 *Inorg. Chem.* **50** 5824
9. (a) Roy D K, Mondal B, Anju R S and Ghosh S 2015 Chemistry of Diruthenium and dirhodium analogues of pentaborane(9): Synthesis and characterization of metal N,S-heterocyclic carbene and B-agostic complexes *Chem. Eur. J*. **21** 3640

   (b) Ramalakshmi R, Saha K, Roy D K, Varghese B, Phukan A K and Ghosh S 2015 New routes to a series of σ-borane/borate complexes of Molybdenum and Ruthenium *Chem. Eur. J*. **21** 17191

   (c) Roy D K, De A, Panda S, Varghese B and Ghosh S 2015 Chemistry of N,S-heterocyclic carbene and metallaboratrane complexes: A new η^3-BCC-borataallyl complex *Chem. Eur. J*. **21** 13732

   (d) Anju R S, Roy D K, Mondal B, Yuvaraj K, Arivazhagan C, Saha K, Varghese B, Ghosh S 2014 Reactivity of diruthenium and dirhodium analogues of pentaborane(9): Agostic versus boratrane complexes *Angew. Chem. Int. Ed.* **53** 2873

   (e) Anju R S, Roy D K, Geetharani K, Mondal B, Varghese B and Ghosh S 2013 A fine tuning of metallaborane to bridged-boryl complex, $[(Cp^*Ru)_2(\mu\text{-}H)(\mu\text{-}CO)(\mu\text{-}Bcat)]$ (cat = $1,2\text{-}O_2C_6H_4$; $Cp^* = \eta^5\text{-}C_5Me_5$) *Dalton Trans.* **42** 12828

   (f) Bose S K, Roy D K, Shankhari P, Yuvaraj K, Mondal B, Sikder A and Ghosh S 2013 Syntheses and characterization of new vinyl-borylene complexes by the hydroboration of alkynes with $[(\mu_3\text{-}BH)(Cp^*RuCO)_2(\mu\text{-}CO)Fe(CO)_3]$ *Chem. Eur. J.* **19** 2337

   (g) Yuvaraj K, Roy D K, Geetharani K, Mondal B, Anju V P, Shankhari P, Ramkumar V and Ghosh S 2013 Chemistry of homo- and heterometallic bridged-borylene complexes *Organometallics* **3** 2705

   (h) Anju R S, Saha K, Mondal B, Dorcet V, Roisnel T, Halet J-F and Ghosh S 2014 Chemistry of diruthenium analogue of pentaborane(9) with heterocumulenes: towards novel trimetallic cubane-type clusters *Inorg. Chem.* **53** 10527
10. (a) Roy D K, Bose S K, Anju R S, Ramkumar V and Ghosh S, 2012 Synthesis and structure of dirhodium analogue of octaborane-12 and decaborane-14 *Inorg. Chem.* **51**, 10715

    (b) Roy D K, Mondal B, Shankhari P, Anju R S, Geetharani K, Mobin S M and Ghosh S 2013 Supraicosahedral polyhedra in metallaboranes: Synthesis and structural characterization of 12-, 15-, and 16-vertex rhodaboranes *Inorg. Chem.* **52** 6705

(c) Roy D K, Bose S K, Anju R S, Mondal B, Ramkumar V and Ghosh S 2013 Boron beyond the icosahedral barrier: A 16-vertex metallaborane *Angew. Chem. Int. Ed.* **52** 3222
(d) Sharmila D, Yuvaraj K, Barik S K, Roy D K, Chakrahari K. K V, Ramalakshmi R, Mondal B, Varghese B and Ghosh S 2013 New heteronuclear bridged borylene complexes that were derived from [{Cp*CoCl}$_2$] and mono-metal carbonyl fragments *Chem. Eur. J*., **19**, 15219

11. Koelle U and Kossakowski J, 1992 Di-μ-chloro-bis[(η^5-pentamethylcyclopentadienyl)chloro ruthenium(III), [Cp*RuCl$_2$]$_2$ and Di-μ-methoxo-bis [(η^5-pentamethylcyclopentadienyl)-diruthenium(II)], [Cp*RuOMe]$_2$ *Inorg. Synth*. **29** 225
12. Lei X, Shang M and Fehlner T P 1999 Chemistry of dimetallaboranes derived from the reaction of [Cp*MCl$_2$]$_2$ with Monoboranes (M = Ru, Rh; Cp* = η^5-C$_5$Me$_5$) *J. Am. Chem. Soc*. **121** 1275
13. Ryschkewitsch G E and Nainan K C 1974 *Inorg. Synth.* **15**, 111
14 Although our aim was to isolate Te incorporated metallahetroborane clusters, we were able to isolate compounds **2** and **3** in poor yields. Note that the ^{11}B NMR of the reaction mixture indicated several boron containing products, however we were unable to isolate any of these due to their instability. Compound **3** was isolated in a very poor yield and all our attempts to reproduce this molecule were failed. Thus, compound **3** was characterized by limited spectroscopic data and an X-ray structural analysis.
15. (a) Sheldrick G M 1997 *SHELXS-97* University of Gottingen: Germany
(b) SIR92, Altornare A, Cascarano G, Giacovazzo C and Guagliardi A 1993 Completion and refinement of crystal structures with SIR92 *J. Appl. Cryst.* **26** 343
(c) Sheldrick G M 1997 *SHELXL-97* University of Gottingen: Germany
16. Frisch M J, Trucks G W, Schlegel H B, Scuseria G E, Robb M A, Cheeseman J R, Scalmani G, Barone V, Mennucci B, Petersson G A, Nakatsuji H, Caricato M, Li X, Hratchian H P, Izmaylov A F, Bloino J, Zheng G, Sonnenberg J L, Hada M, Ehara M, Toyota K, Fukuda R, Hasegawa J, Ishida M, Nakajima T, Honda Y, Kitao O, Nakai H, Vreven T, Montgomery J A. Jr, Peralta J E, Ogliaro F, Bearpark M, Heyd J J, Brothers E, Kudin K N, Staroverov V N, Keith T, Kobayashi R, Normand J, Raghavachari K, Rendell A, Burant J C, Iyengar S S, Tomasi J, Cossi M, Rega N, Millam J M, Klene M, Knox J E, Cross J B, Bakken V, Adamo C, Jaramillo J, Gomperts R, Stratmann R E, Yazyev O, Austin A J, Cammi R, Pomelli C, Ochterski J W, Martin R L, Morokuma K, Zakrzewski V G, Voth G A, Salvador P, Dannenberg J J, Dapprich S, Daniels A D, Farkas O, Foresman J B, Ortiz J V, Cioslowski J and Fox D J 2010 *Gaussian 09*, Revision C.01; Gaussian, Inc.: Wallingford, CT

17. Perdew J P, Burke K and Ernzerhof M 1996 Generalized gradient approximation made simple *Phys. Rev. Lett.* **77** 3865
18. (a) London F 1937 Théorie quantique des courants interatomiques dans les combinaisons aromatiques *J. Phys. Radium.* **8** 397
(b) Ditchfield R 1974 Self-consistent perturbation theory of diamagnetism *Mol. Phys.* **27** 789
(c) Wolinski K, Hinton J F and Pulay P 1990 Efficient implementation of the gauge-independent atomic orbital method for nmr chemical shift calculations *J. Am. Chem. Soc.* **112** 8251
19. (a) Schreckenbach G and Ziegler T 1995 calculation of NMR shielding tensors using gauge-including atomic orbitals and modern density functional theory *J. Phys. Chem.* **99** 606-611
(b) Schreckenbach G and Ziegler T 1997 Calculation of NMR shielding tensors based on density functional theory and a scalar relativistic Pauli-type Hamiltonian. The application to transition metal complexes *Int. J. Quantum Chem.* **61** 899
(c) Schreckenbach G, and Ziegler T 1996 The calculation of NMR shielding tensors based on density functional theory and the frozen-core approximation *Int. J. Quantum Chem.* **60** 753
(d) Wolff S. K and Ziegler T 1998 Calculation of DFT-GIAO NMR shifts with the inclusion of spin-orbit coupling *J. Chem. Phys.* **109** 895
(e) Wolff S K, Ziegler T, van Lenthe E and Baerends E J 1999 Density functional calculations of nuclear magnetic shieldings using the zeroth-order regular approximation (ZORA) for relativistic effects: ZORA nuclear magnetic resonance *J. Chem. Phys.* **110** 7689
20. Zhurko G A *http://www.chemcraftprog.com*.
21. Lu T, Chen F 2012 Multiwfn: a multifunctional wavefunction analyzer *J. Comput. Chem.* **33** 580
22. (a) Bunel E E, Valle L, Jones N L, Carrol P J, Barra C, González M, Munoz N, Visconti G, Aizman A, Manríquez J M 1988 Bis[(pentamethylcyclopentadienyl)metal] pentalenes. A new class of highly delocalized, fused metallocenes *J. Am. Chem. Soc*. **110** 6596
(b) Manríquez J M, Ward M D, Reiff W M, Calabrese J C, Jones N L, P. J. Carroll, E. E. Bunel, J. S. Miller, 1995 Structural and physical properties of delocalized mixed-valent $[Cp^*M(pentalene)M'Cp^*]^{n+}$ and $[Cp^*M(indacene)M'Cp^*]^{n+}$ (M, M' = Fe, Co, Ni; n = 0, 1, 2) Complexes *J. Am. Chem. Soc.* **117** 6182
23. (a) Tait C D, Garner J M, Collman J P, Sattelberger A P and Woodruff W H 1989 Vibrational study of multiply metal-metal bonded ruthenium porphyrin dimers *J. Am. Chem. SOC.* **111** 7806

(b) Poizat O and Sourisseau C 1984 Infrared, Raman, and resonance Raman studies of the ru(2,2'-bpy)$_3^{2+}$ cation in its chloride crystal and as an intercalate in the layered $MnPS_3$ Compound *J. Phys. Chem.* 88 3007

24. Barik S K, Chowdhury M.G, De S, Parameswaran P and Ghosh S 2016 Extended sandwich molecules displaying direct metal–metal bonds *Eur. J. Inorg. Chem.* 4546
25. (a) Boucher B, Ghosh S, Halet J-F, Kahlal S and Saillard J-Y 2012 Bonding and electronic structure of $Cp^*_2Ru_2(B_8H_{14})$, A metallaborane analogue of dinuclear pentalene complexes *J. Organomet. Chem*. **721-722** 167

    (b) Garland M T, Saillard J-Y, Chávez I, Oëlckers B and Manríquez J M 1997 Molecular orbital calculations of binuclear systems of Fe, Co and Ni derivatives of pentalene, s-indacene and as-indacene *J. Mol. Struct*. **390** 199
26. Kudinov A R, Petrovskii P V, Struchkov T, Yanovskii A I and Rybinskaya M I 1991 Synthesis of slipped triple- and tetra-decker cationic ruthenium complexes with the μ, $\eta^5;\eta^6$-indenyl ligand. X-Ray structure of $[(\eta^5\text{-}C_5H_5)Ru(\mu,\eta^5{:}\eta^6\text{-}C_9H_7\text{-}Ru(\eta\text{-}C_5Me_5)]PF_6$ *J. Organomet. Chem.* **421** 91
27. (a) Mercier A, Yeo W C, Chou J, Chaudhuri P D, Bernardinelli G and Kündig E P 2009 Synthesis of highly enantiomerically enriched planar chiral ruthenium complexes via Pd-catalysed asymmetric hydrogenolysis *Chem. Commun*.0 5227.

    (b) Wagschal S, Mercier A and Kundig E P 2013 Enantioselective desymmetrization of 1,2,3-trisubstituted metallocenes by molybdenum-catalyzed asymmetric intraannular ring-closing metathesis *Organometallics* **32** 7133
28. Ghosh S, Beatty A M and Fehlner T P 2003 Transition-metal variation as a probe of the origins of hypoelectronic metallaboranes: eight- and ten-vertex open ruthenaboranes *Angew. Chem. Int. Ed.* **42** 4678
29. Hoffmann R 1982 Building bridges between inorganic and organic chemistry *Angew. Chem. Int. Ed. Engl*. **21** 711–724; *Angew. Chem*. 1982 **94** 725

Table of Contents

Reference number of the paper: JCSC-D-18-00330

Manuscript title: Synthesis and structural characterization of a diruthenium pentalene complex, [Cp*Ru{$(Cp^*Ru)_2B_6H_{14}$}(Cp*Ru)]

Authors: Benson Joseph,[a] Subrat Kumar Barik,[a] Soumya Kumar Sinha,[a] Thierry Roisnel[b] and Sundargopal Ghosh*,[a]

Synopsis of the paper:

Treatment of *nido*-[1,2-$(Cp^*Ru)_2(\mu\text{-}H)_2B_3H_7$] with Te powder led to the isolation of diruthenium pentalene analogue [$(Cp^*Ru)\{(Cp^*Ru)_2B_6H_{14}\}(RuCp^*)$] and a metal indenyl complex [$(Cp^*Ru)_2B_2H_6C_6H_3(CH_3)$].